Optimizing the 3D Plate Shape for Proximal Humerus Fractures

Marilyn Keller, Marcell Krall, James Smith, Hans Clement, Alexander Kerner, Andreas Gradischar, Ute Schäfer, Michael Black, Annelie Weinberg, Sergi Pujades

Optimizing the 3D Plate Shape for Proximal Humerus Fractures

Marilyn Keller[1], Marcell Krall[2], James Smith[2], Hans Clement[2], Alexander M. Kerner[2], Andreas Gradischar[3], Ute Schäfer[2], Michael J. Black[1], Annelie Weinberg[2], and Sergi Pujades[4]

[1] Max Planck Institute for Intelligent Systems, Germany
[2] Medical University of Graz, Austria
[3] CAE Simulation & Solutions GmbH, Austria
[4] Univ. Grenoble Alpes, Inria, CNRS, Grenoble INP, LJK, France

Abstract. To treat bone fractures, implant manufacturers produce 2D anatomically contoured plates. Unfortunately, existing plates only fit a limited segment of the population and/or require manual bending during surgery. Patient-specific implants would provide major benefits such as reducing surgery time and improving treatment outcomes but they are still rare in clinical practice. In this work, we propose a patient-specific design for the long helical 2D PHILOS (Proximal Humeral Internal Locking System) plate, used to treat humerus shaft fractures. Our method automatically creates a custom plate from a CT scan of a patient's bone. We start by designing an optimal plate on a template bone and, with an anatomy-aware registration method, we transfer this optimal design to any bone. In addition, for an arbitrary bone, our method assesses if a given plate is fit for surgery by automatically positioning it on the bone. We use this process to generate a compact set of plate shapes capable of fitting the bones within a given population. This plate set can be pre-printed in advance and readily available, removing the fabrication time between the fracture occurrence and the surgery. Extensive experiments on ex-vivo arms and 3D-printed bones show that the generated plate shapes (personalized and plate-set) faithfully match the individual bone anatomy and are suitable for clinical practice.

Keywords: Personalized plates · 3D printing · ex-vivo evaluation.

1 Introduction

Bone shapes vary significantly across the world's population [1], making the design of personalized medical plates for repairing fractures challenging. Yet patient-specific implants would provide major benefits for surgeons and patients: surgery time would be reduced and treatment outcomes improved. While some plates are malleable enough to be contoured during surgery to improve overall fitness, these are more prone to fatigue failure when compared to rigid pre-contoured plates. But anatomically pre-contoured plates only fit a subset of the

population [2–4], causing malalignment at the fracture site [5]. Even with the extra contouring step during the surgery, the plates do not fit all bone shapes [6].

Our work contributes several key steps to create personalized plates: (i) we first design an optimal PHILOS 3D plate shape for the humerus bone, fulfilling the clinical constraints given by a senior surgeon; (ii) we propose an anatomy-aware transfer of the plate shape into any new bone, resulting in a personalized plate shape; (iii) we propose a method to position an arbitrary plate on an arbitrary bone according to clinical constraints, allowing surgical compatibility to be evaluated; (iv) we leverage the compatibility assessment to obtain a compact set of plates that accommodates a given population of bones; (v) we validate our methodology with extensive experiments on ex-vivo and 3D-printed bones, demonstrating the relevance of the designed personalized plate shapes for the clinical setting; (vi) we make available for research purposes the humerus and plate 3D models, as well as the plate extraction and fitting code[†].

The creation of surgical plates consists of several tasks, which have been partially addressed by the existing state of the art. In Tab. 1 of Sup. Mat. we provide a schematic comparison of how our approach goes beyond existing methods.

Most methods start with a base plate or template that is designed for a specific bone surgery (tibia, humerus, clavicle, etc.) [2, 4, 6–13]. One important step is how to position a given plate on a given bone. Existing approaches are either manual, semi-automatic [2, 3, 7, 11], or fully automatic [4, 9, 10, 12, 14]. Our fully automatic positioning strategy differs from the state of the art as it considers the surrounding anatomy; i.e. to minimize the risk of radial nerve damage, the plate is twisted around the bone so that the proximal end is fixed on the lateral side of the humeral head, and the distal end of the plate to the ventral surface of the humerus [15, 16].

Once the plate is positioned, one needs to evaluate if the plate can be used in surgery. Some works compute plate-to-bone metrics [2, 6, 13, 17], but do not propose a binary decision criterion stating whether the plate is valid for surgery or not. We argue that this binary decision, also provided by existing works [3, 4, 7–9, 11, 12, 14], is important, as aggregate distance numbers can be misleading; e.g. one part of the plate could have a perfect fit but another part could make the plate not suitable for surgery. In our work, we define a three section-based criterion that takes into account the two plate-to-bone fixation regions and the middle plate section that transitions from one fixation region to the other. In addition, we perform a case study evaluation with an expert surgeon, in which the validity of the numerical criterion is confirmed.

Once the plate is positioned on a bone, and the fit evaluated, one can further consider the question of *how to deform the plate to fulfill the fit criterion*. For instance, [6] aims to develop a plate shape to reduce in-situ plate manipulation. They approximate the plate and target bone surfaces by planar sections and measure the bending necessary for each section of the plate to fit the bone surface. In contrast, our approach is similar to the one of [3], in which the plate shape is not deformed after evaluating the fit, but rather directly extracted from

[†] https://humerusplate.is.tue.mpg.de

the shape of an individual bone. We propose a plate transfer strategy that takes into account the matching of anatomic regions. One advantage over existing methods is that our approach simultaneously ensures both: (i) a personalized plate shape matching the bone's shape and (ii) its proper placement.

Prior work proposes a set of plate shapes that, together, can accommodate a range of patients [8, 9]. This set is created by manually modifying an original plate to improve its plate-to-bone distance. We propose an automatic approach in which we first create many plates, and then, with a greedy algorithm, select the plate set that accommodates the most bones.

2 Method

Dataset. To create and evaluate our plate designs, we use a dataset consisting of 97 3D meshes of humerus bones, divided into two groups (A and B). Group A has 54 bones scanned with a FARO laser scanner (25 females and 29 males, 50% Black and 50% White, age range 17 and 45). Group B has 43 Computed Tomography (CT) scans of bones from autotomized body donors. The CT volumes were segmented and cleaned to reconstruct a mesh of the bone. Left-side humerus scans were mirrored along the z-axis to work with right-side humeri only.

Plate design. Given a bone, our goal is to automatically generate an optimal plate shape and determine its position on the bone. The optimality of our plate design is defined by an experienced surgeon, who established fixation points, areas to avoid, and plate-to-bone distance tolerances. These choices were validated by a second expert surgeon. A plate fulfilling these constraints on a bone is considered optimal for surgery. To obtain the plate design we 3D printed 7 bone meshes from our dataset with diverse shapes and asked the surgeon to annotate each bone with a marker. The surgeon indicated the bone areas that should be in contact with an ideal plate and the areas to be avoided (Fig. 1 left). From these annotations, we designed an ideal plate mesh $\mathbf{P_T}$ contoured to a humerus

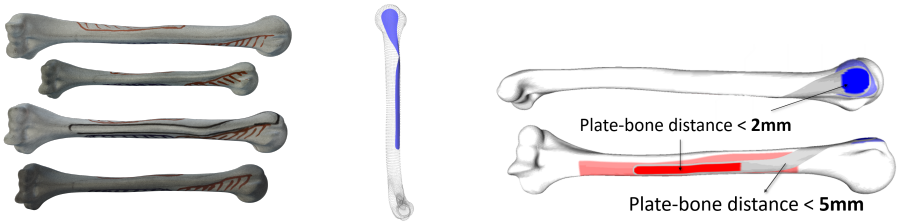

Fig. 1: Left: surgeon annotations showing where the plate should be positioned and areas to be avoided. Middle: the designed plate on the template bone. Right: Plate-on-bone fit criteria. Colors show the vertices defined as the fixation area on the plate (Blue: $\mathcal{P}_h$; Red: $\mathcal{P}_s$) and on the bone (Pale blue: $\mathcal{B}_h$; Pale red: $\mathcal{B}_s$).

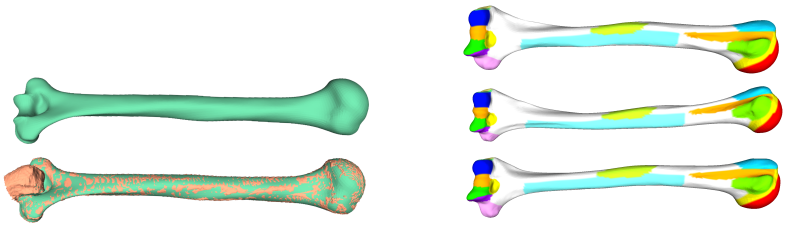

Fig. 2: Left: Registered bone $\mathbf{B}_i$ (green) and superposition to the input scan $\mathcal{S}_i$ (pink). Right: Registrations $\mathbf{B}_i$ to multiple scans. Despite the different individual bends and twists of each bone, the colored anatomic regions are consistent.

template bone mesh $\mathbf{T}$ (Fig. 1 middle). This plate has similar dimensions as the actual INTEOS PROXIMAL HUMERAL PLATE 3.5. Following the surgeon's advise, the plate should not be in contact with the bone at the bone neck level, hence, an offset was added in this region. The fit criteria between a plate and a bone was defined such that the distance between them should not exceed $2mm$ at the fixation points, located at the head $\mathcal{P}_h$ and the shaft $\mathcal{P}_s$, and should be less than $5mm$ in the other regions, with the exception of the plate neck, which must not be in direct contact with the bone (Fig. 1 right).

Bone registration for optimal plate transfer. Once the optimal plate is defined on the template bone, the goal is to register any new bone to the template, by preserving the relevant anatomic regions for the plate fixation. To do so, we adapt the registration technique designed for vertebrae [18] to the humerus.

We first register each bone of set A by optimizing their Eq. 1, 2 and 3 from [18]. Given these initial registrations we build a statistical shape model using principal component analysis (PCA). This model is parameterized with the shape vector $\boldsymbol{\beta}$, and constructs a bone mesh $\mathbf{T}(\boldsymbol{\beta})$: an array of size $N_b \times 3$ containing the mesh vertex positions. Second, we register the whole dataset using the learned bone shape model by minimizing

$$\mathrm{E}(\boldsymbol{\beta}, \mathbf{t}, \mathbf{r}, \mathbf{F}; \mathcal{S}) = E_{p2m}(\mathcal{S}, \mathbf{r} \cdot (\mathbf{T}(\boldsymbol{\beta}) + \mathbf{F}) + \mathbf{t}) + \lambda_{\boldsymbol{\beta}} ||\boldsymbol{\beta}||_2 + \lambda_L \Delta(\mathbf{T}(\boldsymbol{\beta})) \cdot \mathbf{F} \quad (1)$$

where $\mathcal{S}$ denotes the scanned bone mesh, $\mathbf{t}$ and $\mathbf{r}$ are, respectively, the 3D rigid translation and rotation applied to the bone mesh vertices, and $\mathbf{F}$ is a 3D per-vertex offset applied to each mesh vertex. $E_{p2m}(\mathcal{S}, .)$ is the point-to-triangle distance between the scan vertices and the mesh triangles. The function $\Delta(\mathbf{T})$ is the mesh Laplacian operator, which is used to regularize the offsets $\mathbf{F}$. We minimize Eq. (1) in three successive steps: with respect to $(\mathbf{t}, \mathbf{r})$, $\boldsymbol{\beta}$, and $\mathbf{F}$. For each scan $\mathcal{S}_i$ we obtain its corresponding bone registration $\mathbf{B}'_i = \mathbf{T}(\boldsymbol{\beta}) + \mathbf{F}$.

Due to the elongated shape of the humeri and their axial rotation similarity, the registrations $\mathbf{B}'_i$ can contain sliding, i.e. the same vertex does not correspond precisely to the same anatomic location on two different bones. To correct this, we perform a second pass of registration using smooth shells [19] to deform the initial template $\mathbf{T}$ to the surface of $\mathbf{B}'_i$ and we obtain the final bone registrations

$\mathbf{B}_i$ matching the scan $\mathcal{S}_i$ (see Fig. 2 left). Note that smooth shells [19] can not directly register $\mathbf{T}$ to the scans $\mathcal{S}_i$, and the intermediate meshes $\mathbf{B}'_i$ are required.

To validate the bone correspondences we define anatomic regions on the bone template $\mathbf{T}$, and transfer them to all registrations $\mathbf{B}_i$ on a per-vertex index basis. Fig. 2 shows that the annotated anatomic parts are faithfully preserved.

Plate extraction. As the registration process preserves anatomic regions, given a bone registration $\mathbf{B}_i$, we can extract a new optimal plate $\mathbf{P}_i$. For each vertex of the designed plate $\mathbf{P}_\mathbf{T}$ we compute its offset to the template bone $\mathbf{T}$. By applying these offsets to the new bone $\mathbf{B}_i$, we obtain the personalized plate $\mathbf{P}_i$.

Positioning a plate on a bone. Now that we can create personalized plates, we want to study if a created plate can be used for surgery on another bone. For that, given an arbitrary plate $\mathbf{P}_i$ and bone registration $\mathbf{B}_j$, we need to position the plate and determine if it fits. We automate the plate positioning by minimizing the distance between the plate and bone fixation points. We start by computing an initial 3D rigid transformation $\mathbf{r}_0, \mathbf{t}_0$ by optimizing Eq. 2 in Sup. Mat. and then obtaining the final positioning $\mathbf{r}_f, \mathbf{t}_f$ by optimizing Eq. 3 in Sup. Mat. These equations enforce the fixation areas of the plate $\mathcal{P}_h^i$ to match $\mathcal{B}_h^j$ and $\mathcal{P}_s^i$ to match $\mathcal{B}_s^j$ (see Fig. 1 right), while avoiding plate-to-bone inter-penetrations. Once the plate is positioned on the bone, we evaluate the binary fit criteria (see Fig. 1 right) to conclude whether the plate shape is fit for surgery or not.

Plate shapes set. A single plate design can not accommodate the whole population due to its morphological variance [1]. Thus we propose to build a set of plate shapes with a greedy algorithm. The algorithm is summarized in pseudo-code in Alg. 1 of Sup. Mat. Given a bone dataset, we start by creating as many personalized plates as bones. Then, for each plate we use the previous optimization to determine how many bones it accommodates, i.e how well a plate shape generalizes to different bones. We then select the plate that fits most bones and remove the plate and the fitted bones from the current sets. We iterate until no bones are left. The result is an ordered plate-set that accommodates the input bone dataset.

3 Experiments

3.1 Numerical evaluations

Bone registration accuracy. We validate that our registrations $\mathbf{B}_i$ accurately match the scans $\mathcal{S}_i$ by computing the mean distance (MD) between each registration to the closest vertex in the scan. We obtain a MD of 0.08 mm (std=0.04) for group A, and a MD of 0.27 mm (std=0.55) for group B. For both sets, the registered bones match the scans with sub-millimeter accuracy. In addition, all distances are less than 1mm on the surface where the plate is positioned (Fig. 3 left).

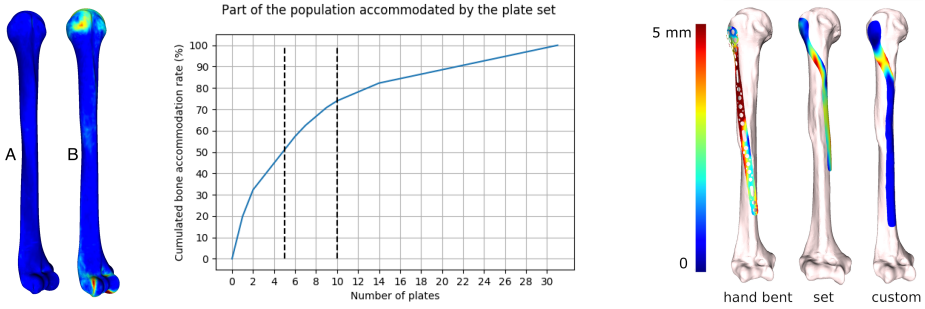

Fig. 3: Left: Per vertex max distance between the registrations $\mathbf{B}_i$ and scans $\mathcal{S}$ for bone set A (left) and B (right). Blue (0 mm) to red (1 mm). Max distances are higher for bone set B because of their lower scan quality (segmentation artifacts). Middle: Accommodation percentage as a function of the number of plates. Right: Plate-to-bone distance for three plates: surgeon's hand bent, best from the plate set, and custom plate. Blue (0mm) to red (5mm or more).

Plate set coverage. One application of our design is that it can generate a plate set that could be preprinted in the hospital and be readily available for immediate use. Using our greedy algorithm on our bone dataset, a set $\mathcal{P}_S^{N=5}$ made of the first 5 plates accommodates already 51.04% of the bones and $\mathcal{P}_S^{N=10}$ accommodates 73.96% (Fig. 3 middle). In Sec. 4 we discuss how this coverage could be improved.

3.2 Ex-vivo evaluations

Comparison with state-of-the-art plates. We CT-scanned an isolated bone (not included in the original dataset) and asked a surgeon to manually contour a state-of-the-art plate, as done in clinical practice. We compare it to the *custom plate* $\mathbf{P}_C$ and the best *set plate* $\mathbf{P}_S$ by computing the plate-to-bone distances (Fig. 3 right). The proposed plates are clearly closer to the bone than the hand-contoured plate. This proximity is known to be beneficial for bone recovery [20]. While $\mathbf{P}_S$ is less accurate than the custom plate - and shorter, as it was generated from a shorter bone - the surgeon considered the plate and its placement as suitable. This experiment reveals the difficulty of closely fitting the bone by manually bending a plate and the benefit of the proposed design.

Ex-vivo surgery. We performed an ex-vivo experiment on a cadaveric arm, mimicking an actual minimally-invasive surgical operation setting. One goal was to test whether the designed 3D plates can be properly inserted along the bone under the muscles. We CT-scanned 3 cadaveric arms (not included in the original dataset), reconstructed the bone scans and registered them to obtain $\mathbf{B}_1$, $\mathbf{B}_2$ and $\mathbf{B}_3$. For each bone we generated and 3D printed their custom plate $\mathbf{P}_C^{1,2,3}$ and the best fitting set plate $\mathbf{P}_S^{1,2,3}$. The plates were drilled and coated with metallic paint to be visible on the CT scan. During the experiment, the plates

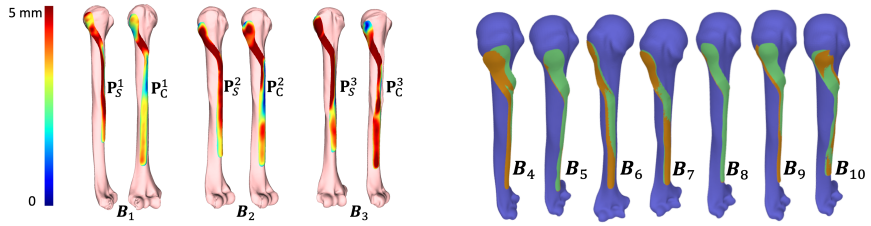

Fig. 4: Left: Color-coded plate-to-bone distances (blue: 0 mm; red: $\geq$ 5 mm) for the set plate and custom plate on bones $\mathbf{B}_1$, $\mathbf{B}_2$, and $\mathbf{B}_3$. Right: Placement of the 3D printed plates $\mathbf{P}_S$ on the corresponding 3D printed bone: green: algorithm's placement; orange: the surgeon's placement.

were inserted in the cadaver arm, as it would be done in a standard operation, and fixed to the humerus with screws. For the 3 bones, the surgeon estimated that the fit of both the custom and set plates was satisfactory. He noted that the surface roughness of the 3D print and metallic coating was too high, making the plate hard to slide across the humerus into place.

We CT-scanned each plate screwed to the bone and used the scans to asses the fit quality. Fig. 4 left shows the plate-to-bone distances for each bone. The plate $\mathbf{P}_C^1$ fits closely on the proximal side near the sulcus bicipitalis. For $\mathbf{P}_C^2$ and $\mathbf{P}_C^3$ the fits are not as good as $\mathbf{P}_C^1$. This was credited to a handling/alignment issue raised by the surgeon. Consequently, greater deviation in alignment is seen on the distal end of the bone on the lateral side. There is also a greater distance between the ventral part of the plate and the sulcus bicipitalis. The plate is too lateral on the humerus. In each case, the surgeon found the custom plate better. The limit in terms of fit was mainly attributed to the operative process rather than to the plate shape itself. The surgeon was satisfied with the 6 fits and noted that the 3D-printed plates were less stiff than the commercial plates he usually uses, making them harder to manipulate.

3.3 Evaluations with 3D-printed bones

To further evaluate our design, we generated 7 bones $\{\mathbf{B}_i\}_{i\in[4;10]}$. $\mathbf{B}_7$ is the mean bone shape and the 6 others are generated by uniformly sampling the bone PCA space $\mathcal{B}$ ($\beta \in \{-2, 2\}$) in the first 3 PCA dimensions. For each bone, we 3D printed its custom plate, $\mathbf{P}_C$, and the best set plate, $\mathbf{P}_S$, from the plate-set.

First, we presented pairs of bones and plates to the surgeon and asked whether they were fit for surgical use. Then, we asked them to position the plates on the 3D bones to evaluate our positioning strategy. Last, to evaluate the adequacy of a plate set, we presented one bone to the surgeon and asked them to choose the best plate from the set.

Ready-for-surgery evaluation. For each bone $\mathbf{B}_i$, the surgeon considered both plates as candidates and evaluated if their shape was suitable for surgery. The

surgeon stated that 100% of the plates were fit for surgery and that the custom plates $\mathbf{P}_C$ were always clearly better fitting than the plates $\mathbf{P}_S$ from the set.

Positioning evaluation. To evaluate the plate positioning computed by our algorithm, we compare it to the surgeon's positioning. We asked the surgeon to position the set plates $\mathbf{P}_S$ on each bone, secured them with blue tack and scanned the whole with a FARO hand scanner. Fig. 4 right shows the overlay of both positions of the used plate for each bone. For most bones, the placement of the plate by the surgeon and the algorithm were very similar. The differences can be explained as there are multiple plate positions that fit. Both placements (orange and green), even in the most dissimilar case (first bone in Fig. 4 right) were considered correct by the surgeon.

Choosing from the plate set. Our algorithm iteratively positions the plates $\mathbf{P}_S^i$ from $i = 0$ to $i = N$ and picks the best-fitting plate, so we asked the surgeon to perform a similar trial-and-error task to evaluate the relevance of our plate set.

Out of the 7 bones, the surgeon only chose the same plate as our algorithm for two of them ($\mathbf{B}_7$ and $\mathbf{B}_{10}$). For the other cases, the surgeon compared his selection to the algorithms' choice and confirmed that both plates were fit for surgery: different plates with slightly different placements can work for the same bone. Most interestingly, some plates selected by the surgeon did not fit the bone according to the strict numeric fit criteria. We discuss this finding in the next section. The surgeon noted that the plates of our set were always preferred over the state-of-the-art plates.

4 Conclusions, take-aways and future work

Conclusion. We propose to automatically generate a custom humerus plate that specifically matches the 3D shape of a bone and specifically meets the requirements of a surgeon for minimally invasive surgery. We also generate a set of plate shapes that accommodates a given bone population. We extensively evaluate our approach on cadaverous arms and 3D printed bones.

Experimental takeaways. All the proposed plates (individual and set plate) match the shape of the bones, while the individual ones are considered the best by the surgeon. Furthermore, our experiments show the importance of evaluating on 3D-printed bones and ex-vivo arms. With the former, the surgeon can easily assess the plate-to-bone fit. With the latter, the insertion procedure can affect the plate placement. Moreover, our results on 3D printed bones argue for a relaxation of the *theoretical* fitting constraints: the plate-to-bone distance could be higher in some areas while still obtaining a proper surgical fit. Loosening the tolerances would allow more bones to be fit with the same plates and potentially the number of plates required in the plate set could be further reduced.

Future work. To reach actual clinical use, two elements need consideration: (i) the current method takes as input the shape of a healthy bone, whereas patients have a fracture. One could perform a CT scan of the other arm and generate the symmetric bone or leverage methods that reconstruct a full bone from partial observations [21]. (ii) Our work focuses on the geometric design of the plate but does not consider the physical properties of the plate, such as thickness and stiffness. Future work should optimize these physical properties for the stresses that the plate must endure, e.g. using finite element methods.

5 Acknowledgements

This work was supported by the project CAMed (COMET K- Project 871132) which is funded by the Austrian Federal Ministry of Transport, Innovation and Technology (BMVIT) and the Austrian Federal Ministry for Digital and Economic Affairs (BMDW) and the Styrian Business Promotion Agency (SFG). Michael J. Black (MJB) has received research gift funds from Adobe, Intel, Nvidia, Meta/Facebook, and Amazon. MJB has financial interests in Amazon, Datagen Technologies, and Meshcapade GmbH. MJB's research was performed solely at MPI.

For the scanned humerus dataset, we acknowledge Dr. Brian Corner, Dr. Jeff Hudson who did the scanning, and the Cleveland Museum of Natural History Physical Anthropology Dept for access to the Hamann-Todd human skeletal collection. We also thank Anja Gieringer for the bone CT scans and Karoline Seibert at Hofer GmbH & Co KG, Fürstenfeld, Austria for the 3D printing of bones and plates.

References

1. White, T.D., Folkens, P.A.: The human bone manual. Elsevier (2005)
2. Goyal, K.S., Skalak, A.S., Marcus, R.E., Vallier, H.A., Cooperman, D.R.: Analysis of anatomic periarticular tibial plate fit on normal adults. Clinical Orthopaedics and Related Research (1976-2007) **461**, 245–257 (2007)
3. Schmutz, B., Rathnayaka, K., Albrecht, T.: Anatomical fitting of a plate shape directly derived from a 3D statistical bone model of the tibia. Journal of clinical orthopaedics and trauma **10**, S236–S241 (2019)
4. Kozic, N., Weber, S., Büchler, P., Lutz, C., Reimers, N., Ballester, M.Á.G., Reyes, M.: Optimisation of orthopaedic implant design using statistical shape space analysis based on level sets. Medical image analysis **14**(3), 265–275 (2010)
5. Hwang, J.H., Oh, J.K., Oh, C.W., Yoon, Y.C., Choi, H.W.: Mismatch of anatomically pre-shaped locking plate on asian femurs could lead to malalignment in the minimally invasive plating of distal femoral fractures: a cadaveric study. Archives of orthopaedic and trauma surgery **132**(1), 51–56 (2012)
6. Bou-Sleiman, H., Ritacco, L.E., Nolte, L.P., Reyes, M.: Minimization of intraoperative shaping of orthopaedic fixation plates: a population-based design. In: International Conference on Medical Image Computing and Computer-Assisted Intervention. pp. 409–416. Springer (2011)

7. Schmutz, B., Wullschleger, M.E., Kim, H., Noser, H., Schütz, M.A.: Fit assessment of anatomic plates for the distal medial tibia. Journal of orthopaedic trauma **22**(4), 258–263 (2008)
8. Schmutz, B., Wullschleger, M.E., Noser, H., Barry, M., Meek, J., Schütz, M.A.: Fit optimisation of a distal medial tibia plate. Computer Methods in Biomechanics and Biomedical Engineering **14**(04), 359–364 (2011)
9. Harith, H., Schmutz, B., Malekani, J., Schuetz, M.A., Yarlagadda, P.K.: Can we safely deform a plate to fit every bone? Population-based fit assessment and finite element deformation of a distal tibial plate. Medical engineering & physics **38**(3), 280–285 (2016)
10. Carrillo, F., Vlachopoulos, L., Schweizer, A., Nagy, L., Snedeker, J., Fürnstahl, P.: A time saver: Optimization approach for the fully automatic 3d planning of forearm osteotomies. In: Medical Image Computing and Computer-Assisted Intervention-MICCAI 2017: 20th International Conference, Quebec City, QC, Canada, September 11-13, 2017, Proceedings, Part II 20. pp. 488–496. Springer (2017)
11. Wu, X., Xia, Q., Rong, K., Gan, M., Wen, G., Yin, X., Yang, H.: Preliminary exploration of a quantitative assessment index for the matching performance of anatomical bone plates using computer. Journal of Orthopaedic Surgery and Research **14**(1), 1–8 (2019)
12. Tkany, L., Hofstätter, B., Petersik, A., Miehling, J., Wartzack, S., Sesselmann, S.: New design process for anatomically enhanced osteosynthesis plates. Journal of Orthopaedic Research **37**(7), 1508–1517 (2019)
13. Zenker, M., Theodorou, E., Andermatt, D., Winkler, R., Hoyen, H.A., Jaeger, M., Jiang, C., Lambert, S., Nijs, S., Fontana, A.D.: Quantifying osteosynthesis plate prominence–mathematical definitions and case study on a clavicle plate. Computer Methods in Biomechanics and Biomedical Engineering pp. 1–10 (2022)
14. Schulz, A.P., Reimers, N., Wipf, F., Vallotton, M., Bonaretti, S., Kozic, N., Reyes, M., Kienast, B.J.: Evidence based development of a novel lateral fibula plate (variAx fibula) using a real CT bone data based optimization process during device development. The Open Orthopaedics Journal **6**, 1–7 (2012)
15. Gill, D.R., Torchia, M.E.: The spiral compression plate for proximal humeral shaft nonunion: a case report and description of a new technique. Journal of orthopaedic trauma **13**(2), 141–144 (1999)
16. Da Silva, T., Rummel, F., Knop, C., Merkle, T.: Comparing iatrogenic radial nerve lesions in humeral shaft fractures treated with helical or straight philos plates: a 10-year retrospective cohort study of 62 cases. Archives of Orthopaedic and Trauma Surgery **140**(12), 1931–1937 (2020)
17. Petersik, A., Homeier, A., Hoare, S.G., von Oldenburg, G., Gottschling, H., Schröder, M., Burgkart, R.: A numeric approach for anatomic plate design. Injury **49**, S96–S101 (2018)
18. Meng, D., Keller, M., Boyer, E., Black, M., Pujades, S.: Learning a Statistical Full Spine Model from Partial Observations. In: Shape in Medical Imaging. ShapeMI 2020, Lecture Notes in Computer Science, vol. 12474, pp. 122–133. Springer (Oct 2020). https://doi.org/10.1007/978-3-030-61056-2_10, https://hal.inria.fr/hal-02983880
19. Eisenberger, M., Lahner, Z., Cremers, D.: Smooth shells: Multi-scale shape registration with functional maps. In: Proceedings of the IEEE/CVF Conference on Computer Vision and Pattern Recognition. pp. 12265–12274 (2020)
20. Ahmad, M., Nanda, R., Bajwa, A., Candal-Couto, J., Green, S., Hui, A.: Biomechanical testing of the locking compression plate: when does the distance between

bone and implant significantly reduce construct stability? Injury **38**(3), 358–364 (2007)
21. Meng, D., Keller, M., Boyer, E., Black, M., Pujades, S.: Learning a statistical full spine model from partial observations. In: International Workshop on Shape in Medical Imaging. pp. 122–133. Springer (2020)